Synthesis and characterization of functionalized carbon nanotubes employing cobalt nitrate and acetone by using spray pyrolysis deposition technique

Jorge A. Gómez, Alfredo Márquez, M. Avalos-Borja, Antonino Pérez, A. Duarte-Moller and E. Orrantia Borunda.

Abstract

Recently, alcohols and ketones have been employed to sensitize CNT by CVD. A study has shown the importance of the chemical nature of those carbon precursors on the characteristics of the CNTs (carbon nanotubes) obtained. In the present work, we show the influence of the catalyst employed on the synthesis of functionalized multiwall carbon nanotubes (MWCNTs) utilizing acetone as carbon source and cobalt nitrate $Co(NO_3)_2$ has as catalyst.

Introduction

For the synthesis of carbon nanotubes are seeking a simple and economical method. It has been reported in the literature the use of carbon sources for the synthesis of carbon nanotubes as acetylene [1-4], toluene [5], n-hexane, benzene and cyclopentadiene [6], etc., And ultimately alcohols have been used [7-13]. Montoro et al. [13] reported in a large comparative study that acetone is the best candidate to synthesize multiwall carbon nanotubes, based on this type of analysis.

Respect to the catalysts used for the synthesis of the NTCs (Carbon nanotubes) are used some ceramics such as alumina, impregnated in some salts such as nitrates of cobalt-nickel, cobalt and manganese acetates, various transition pure metals such as Iron, Cobalt, Zinc, Ruthenium/ Palladium, Co Na-Y, etc. Inoue and Kikuchi [9] explained that cobalt, compared with iron, exhibits a poor interaction with the coal, but better to

decompose ethanol. This also shows a preference between catalysts for the nucleation and growth according Huh et al. [14] and Shin et al. 15], as well as the size of the particle. Furthermore Liu et al. [16] prepared composites based on polyamide and functionalized carbon nanotubes.

In this work, we select acetone as a carbon source and nitrate of cobalt as a catalyst, which will assess their performance in the synthesis of carbon nanotubes along the tube to spray synthesis, and it will also consider the ketone and nitrate groups from the breakdown of these compounds on the functionalization of multiwall carbon nanotubes.

Experimental details

An aqueous solution of acetone 99.6% purity supplied by JT Baker and cobalt nitrate hexahydrate ($Co(NO_3)_2 \cdot 6H_2O$) at 99.0% purity supplied by Acros Organic that has been used as catalyst. This solution was held at a concentration of 1 × 10-4-ml-1 moles of catalyst on acetone (97.55 wt% acetone and 2.44% by weight of nitrate cobalt). It uses a flow of argon at 99.999% purity as carrier gas.

Figure 1 shows the fogging system pyrolytic used for synthesis of nanotubes of coal multilayer MWCNTs of acetone-cobalt, in turn shown the connection form of equipment used to measure inlet temperature, well as the composition of the flue gases. For *t* his synthesis was used Thermolyne ® cylindrical furnace 40cm in length. In a vicor tube of 45cm in length and 9mm internal diameter used as the substrate placed inside the oven. Figure 2 shows the division of the zones of the tube considered in the analysis after the reaction has been carried out, the zone upstream is the part at the entry of the tube, in this zone the acetone and the catalyst, which they have previously been

nebulized, enter to vicor tube and this is where the decomposition reaction begins that continues along the tube, First isotherm zone, zone isotherm Second, are the two middle parts of the tube and downstream zone is the part of the exhaust gas resulting from the decomposition and synthesis of NTCs.

We used a set of gas analyzers CGT-7000 (Infrared gas analyzer) and the NOA-7000 (NOx, O_2 Gas Analyzer). In order to monitor the exit of the product gases of the reaction to the exit of the vicor tube during the synthesis. In addition a thermocouple was attached in the area to monitor UPSTREAM ZONE initial temperature at the entrance of the tube and this is where our experience shows the best carbon nanotubes synthesized in this technique, (Figure 1).

For the synthesis of nanotubes we selected four temperatures 700°C, 800°C, 900°C, 1000°C and keeping constant during the synthesis phase. During the preheating phase, we applied a small argon flow of 0.8L-min-1. Once the furnace temperature had been reached, the solution was applied through a spray mist whose speed is 1ml/min of acetone under an argon flow of 2.5L-min-1. 20 ml of acetone catalysts was nebulized into the vicor tube with a flow of 3.5L-min-1. The assembly was allowed to cool to room temperature keeping during this process a flow of argon 0.8L/min. The vicor tube was cut into four sections to be named these sections to the analysis phase have been called according to his position upstream zone, first and second downstream Isothermal zones and each of 7.5cm in length.

In order to observe the growth of carbon nanotubes a small segment of each of these parts have been extracted and analyzed using a scanning microscope JEOL JSM-7401F. Subsequently each of these segments was separately immersed in an

acidic solution (1:3) nitric/sulfuric [17] and extracted carbon nanotubes from the substrate by vicor ultrasonic treatment. To remove acid residues were washed with distilled water and tri several rinses in acetone. Finished the cleanup phase was finally suspended in acetone itself.

A small drop of this solution was placed on a copper grid with carbon membrane to be observed in a transmission microscope Tecnai F30 to 200kV. The analysis of the presence of nanotubes and waste took place in the PAN analytical X-ray spectrometer, model X'Pert PRO MPD X'Celerator detector. For the analysis of the functionalization of carbon nanotubes got the liquid solution in a range close to 70°C by day and a half to evaporate the solvent for suspension. After several washings with methanol, was placed a small drop of the suspension in a Thermo Scientific Nicolet FT IR 6700. To observe the spectrum, these analyses were performed only on the upstream zone area synthesized at 900° given the amount of sample collected from all others was not enough for further analysis.

Results and discussions

(a) Decomposition of cobalt nitrate hexahydrate

In Figure 3, the cobalt oxide residues were identified at the end of the test TGA/DSC, and the percentages of weight loss in water, nitrogen oxides, to be corroborated from the calculations in HSC 5.1 [18] of the percentages shown in Table 1. We observe a phase denitrification about 25% near 180°C, after this phase, the system no longer holds water in its structure and then begins des nitrification stage, this leads to the loss in weight almost 35% between 182°C to 275°C, however, we see finally a final residue of 30.37% corresponding to cobalt oxide was detected by XRD analysis,

Figure 4. It was verified through a thermodynamic model for HSC, which shows the simulated results for the ΔG training. The first reaction predicts the dehydration process:

$$Co(NO_3)_2 6H_2O \rightarrow Co(NO_3)_2 + 6H_2O. \qquad (1).$$

The second (Reaction 2) predicts the loss of cobalt nitrate:

$$Co(NO_3)_2 \rightarrow CoO + NO + NO_2 + O_2. \qquad (2)$$

We can say that the production of NO and NO_2 occurs, given that it was possible to detect its presence (Table 2), these results were measured experimentally during the synthesis of NTCs. Note also that the reaction was carried out effectively begins after the 300°C as predicted in Figure 5.

(b) Generation of CO, CO_2, H_2O to form carbon nanotubes

Similarly, Figure 6 illustrates the results of the simulation graphs showing the formation ΔG predicting possible decomposition of the acetone. The reaction proposal was made based on experimental data contained in Table 3 was taken to the exit of the vicor tube during a small complementary experiment about the decomposition of pure acetone. This table shows the presence of carbon monoxide and whose concentration increases with temperature:

$$C_3H_6O \rightarrow CO + 2C + 3H_2\uparrow. \qquad (3)$$

Inside the vicor tube there is a temperature gradient as the tubular furnace temperature gradient that varies from the inlet tube to the middle area where the furnace thermocouple. Now we can say that the decomposition reaction of acetone starts to occur around 100°C almost at the entrance of the tube. Complementarily note

in Figure 3 that while the acetone is beginning to decompose to CO and hydrogen, cobalt nitrate is just beginning to lose water. This water vapor, CO and CO_2 is formed as extra hydrogen Nashibulin et al. [19]. The unreacted CO (Table 3) reduced cobalt oxides [20] and begins to generate cobalt carbides are the initial steps for the synthesis of carbon nanotubes by disproportionalization CO [19, 20] which is the source of carbon for the synthesis of carbon nanotubes. Nashibulin explained that the CO_2 and water "clean" the precipitated amorphous carbon on the surface of the nanotubes, as well as preventing the inhibition of the catalytic particle and maintaining the conditions of formation of nanotubes by disproportionalization and hydrogenation.

As mentioned, the decomposition reaction begins to occur once the nebulized solution enters the tube synthesis. The catalyst particles begin to grow from the inlet to the outlet vicor tube (Figure 2), with a particle size of smaller cobalt at the entrance of the tube and as it moves over the tube, these particle sizes are increasingly large, this is due by the time you have the nuclear cobalt particles. In accordance with what stated by Shin et al. [15], the systematic morphology of the catalyst, such as the grain size and density of the transition metals control the diameter and length of the nanotubes, which explains the differences in size and morphology of the nanotubes synthesized at 800°C.

Figure 8 shows SEM images of the four zones synthesized at 800°C, and according to Figure 2. Also shown for nanotube formation in the four areas of vicor tube. 8a in the image area corresponding to the upstream zone, where observed thinner and longer nanotubes with small protrusions attached to hemispherical surface. These bumps are most likely composed of amorphous carbon. In Figure 8b, we observe the isothermal zone and the smaller nanotubes and a bit thicker than in the previous area

but in fewer. Figure 8c shows the second isothermal zone, it is observed that the nanotubes are slightly shorter than in the first Isothermal zone, but thicker than in the upstream zone. Finally, the down isotherm zone, see Figure 8d carbon nanotubes thicker than the last three areas, but in smaller numbers. Some of these nanotubes appear to be linked to form a “Y”.

Figure 9 illustrates the synthesis of NTCs at 900°C, we observed formation of carbon nanotubes only in the upstream zone, while in the other three areas (First isotherm zone, second isotherm zone, and downstream zone) tube vicor, there were no structures similar to a nanotube. Indeed, we observe in Figure 9a, orderly and uniform growth of these nanotubes, has occurred only in the upstream zone at 900°C. For the first isotherm zone, Figure 9b was observed certain amorphous carbon conglomerations almost 300nm in diameter and about one micron in length. For the second isotherm zone 9C, were found scarce conglomerations spherical of near 200nm radio of amorphous carbon. For upstreams zone, 9D, there was no structure whatsoever. Figure 10 illustrates the forest of nanotubes obtained in the upstream zone at 900°C where you can appreciate the orderly growth of the same. It is important framing that these nanotubes were longer, fine and more numerous than those synthesized to 800°C. Nashibulin et al. showed that the reactions that keep the formation of carbon nanotubes (disproportionalization and hydrogenation) are extinguished at temperatures above the 908°C due to the dominant role of these reversible reactions. Due to this fact, we observe that the formation of nanotubes along the tube at 800°C was in all four segments vicor tube, whereas in the 900°C satisfactory growth occurred only in the first zone (Figures 9 and 10). Given that there were no carbon nanotubes at 1000°.

Figure 10 shows a TEM image of multiwall carbon nanotubes synthesized, which shows the internal structure containing a small portion of the catalyst, it is presumably of cobalt or carbide. One can also observe a thin outer layer of amorphous carbon which covers it. In Figure 11, you can see the FT IR spectrum where there is possible evidence of groups (-NO_2) near the wave numbers 1640 and 1620. It also can be observed for evidence of ketone groups close to the wave numbers 1725 and 1705. Hanming Lui [quote] synthesized functionalized nanotubes where the results are similar in morphology of carbon nanotubes. Hay to change the image in TEM and possibly check the EDS mapping functional groups.

Conclusions

The synthesis of carbon nanotubes from cobalt nitrate and acetone using the method of spray pirólis, resulted in addition to the carbon source and metallic cobalt as a catalyst, water and CO_2 to remain in good condition formation of carbon nanotubes. An incomplete decomposition reaction of these two compounds resulted in several functional groups adhere to the graphemic structure of the nanotubes and the little that was possible with FT IR detection.

The water produced by the same cobalt nitrate participates in the formation of CO_2 from CO decomposition product of acetone. We have been proposed as additional work the hydration control of cobalt nitrate to observe the effect of growth and quality of carbon nanotubes. In addition to a change in the way of collection of catalyst particles to get the most use of reagents and increase the production of multiwall carbon nanotubes.

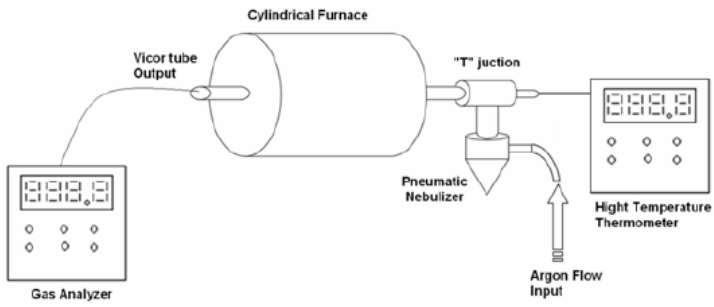

Figure 1. Spray pyrolysis system with a gas measurements equipment employed.

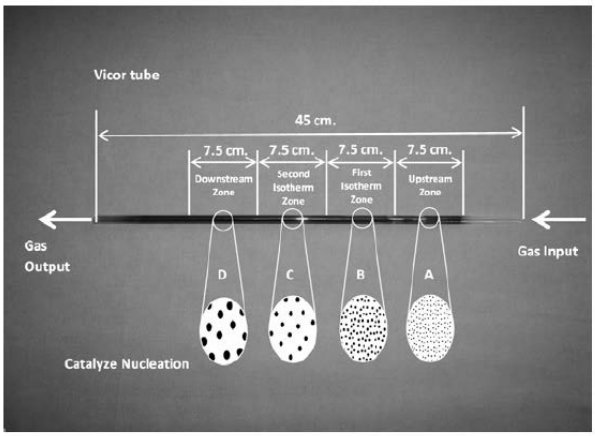

Figure 2. Vicor tube image, with measurements and identification of zones.

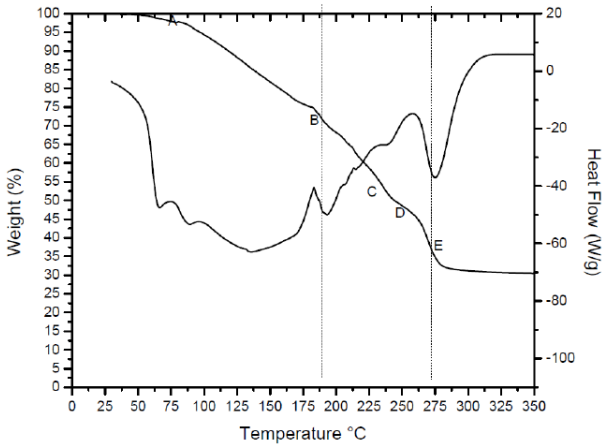

Figure 3. Cobalt nitrate decomposition DSC analysis.

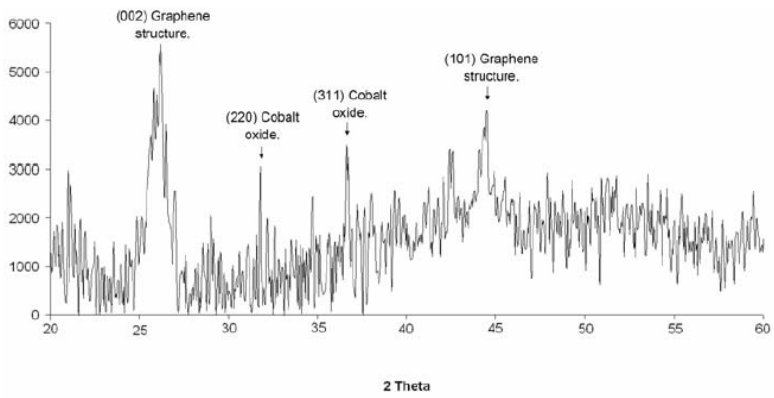

Figure 4. RX diffraction of carbon nanotubes.

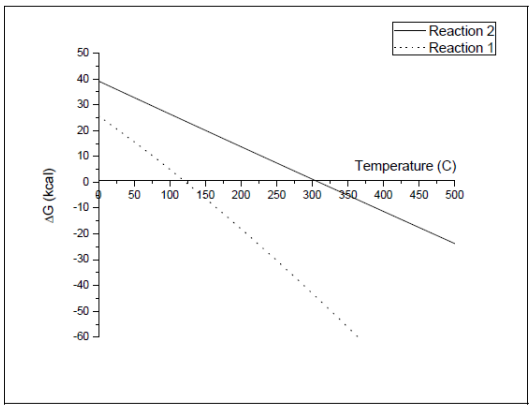

Figure 5. Energy formation ΔG analysis of cobalt nitrate dehydration and decomposition.

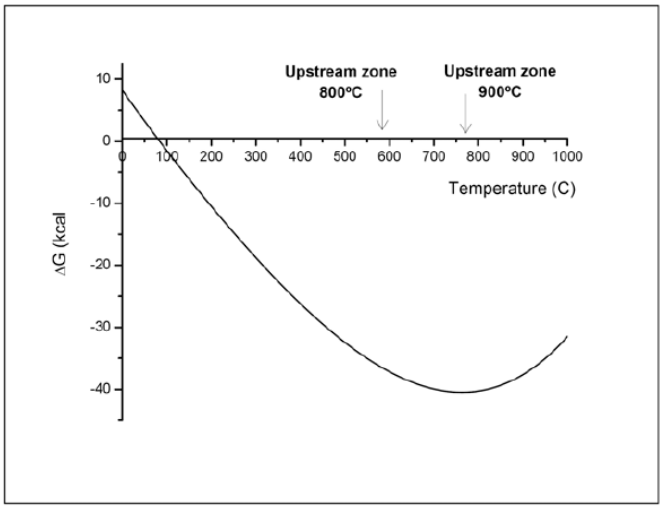

Figure 6. Energy formation ΔG analysis of acetone decomposition.

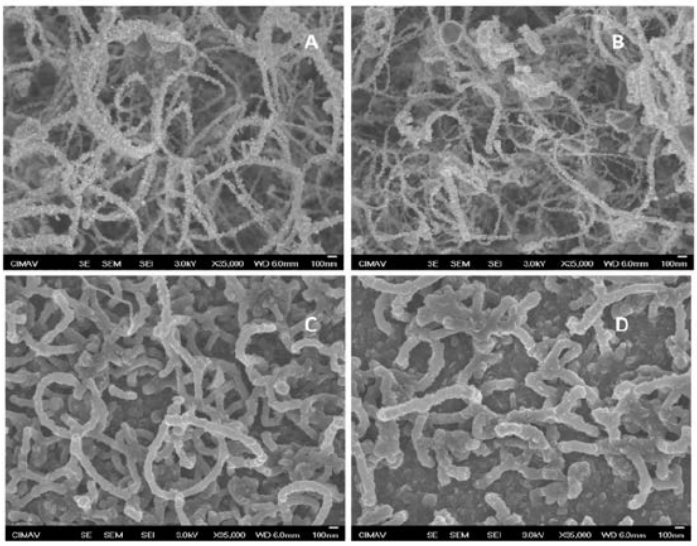

Figure 7. SEM images carbon nanotubes synthesized to 800°C of the four zones analyzed.

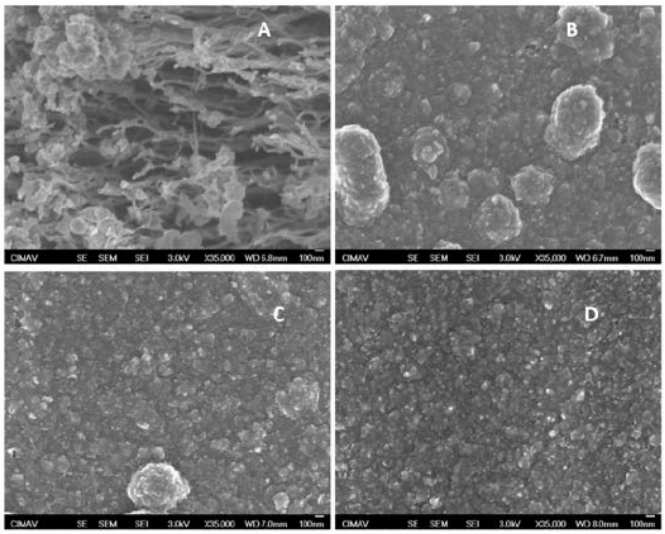

Figure 8. SEM images carbon nanotubes synthesized to 900°C of the four zones analyzed.

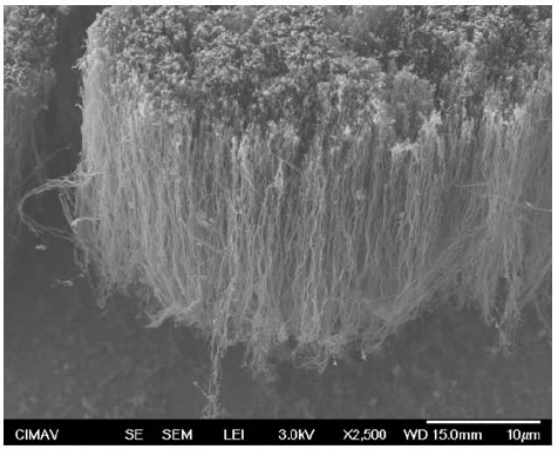

Figure 9. Well aligned forest of carbon nanotubes synthesized to 900°C for the upstream zone.

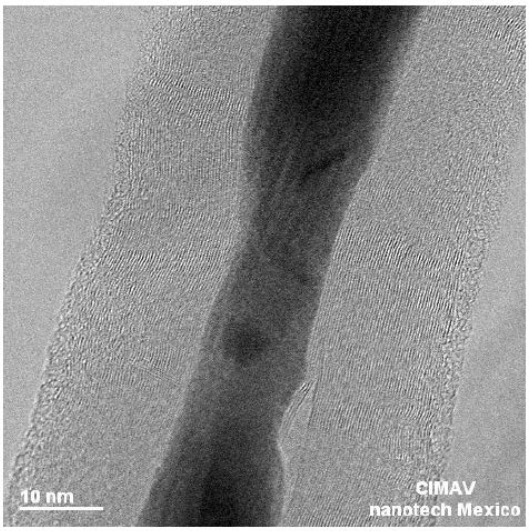

Figure 10. TEM images of carbon nanotubes of first isothermal zone synthesized to 900°C.

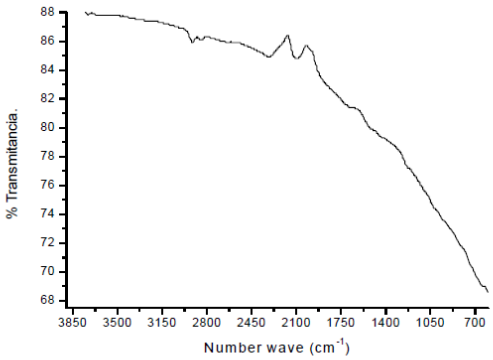

Figure 11. FT IR image of carbon nanotubes of first isothermal zone.

Table 1. Decomposition of cobalt nitrate (from 25 to 400°C)

Weight Loss (%)		
Formula	**Percent weight**	**Acumulative %**
$Co(NO_3)_2 * 6H_2O$	100	-
H_2O	37.140	62.86
NO_2	15.808	47.052
O_2	10.995	-
NO	10.310	25.747
CoO	25.747	

Table 2. Cobalt nitrate-acetone decomposition weight loss

Cobalt nitrate decomposition during reaction			
Oven Temp.	**Spraying temperature**	**NO_x ppm**	**NO ppm**
800°C	30°C	151.7	173.3
900°C	30°C	116.4	123.8

Table 3. Experimental percentage weight of propanone decomposition

Acetone decomposition				
Oven Temp.	**Spraying temperature**	**Upstream Zone Temperature**	**CO ppm**	**CO_2 Vol%**
800°C	30°C	560°C	1881	0.02
900°C	30°C	774°C	5754	0.05

References

[1] S. Seelan, D. W. Hwang, L. P. Hwang and A. K. Sinha, Synthesis of multiwalled carbon nanotubes by high-temperature vacuum annealing of amorphous carbon, Vacuum 75 (2004), 105-109.

[2] Zong-Xiang Xu, Jing-Dong Lin, V. A. L. Roy, Yan Ou and Dai-Wei Liao, Catalytic synthesis of carbon nanotubes and carbon spheres using Kaolin supported catalyst, Materials Science and Engineering B 123 (2005), 102-106.

[3] E. Terrado, M. Redrado, E. Muñoz, W. K. Maser, A. M. Benito and M. T. Martínez, Carbon nanotube growth on cobalt-sprayed substrates by thermal CVD,

Materials Science and Engineering C 26 (2006), 1185-1188.

[4] Seongyop Lim, Atsushi Shimitzu, Seong Ho Yoon, Yozo Koral and Isao Mochida, High yield preparation of tubular carbon nanofibers over supported Co-Mo catalyst, Carbon 42 (2004), 1279-1283.

[5] G. Alonso-Nuñez, A. M. Valenzuela-Muñiz, F. Paraguay-Delgado, A. Aguilar and Y. Verde, New organometallic precursor catalysts applied to MWCNT synthesis by spray-pirolysis, Optical Materials 29 (2006), 134-139.

[6] Kiyoshi Otsuka, Yoshimune Abe, Nobuhiro Kanai, Yoji Kobayashi, Sakae Takenaka and Eishi Tanabe, Synthesis of carbon nanotubes on Ni/Carbon catgalyst under mild conditions, Carbon 42 (2004), 727-736.

[7] A. Gruüneis, M. H. Rümmeli, C. Kramberger, A. Barreiro, T. Pichler, R. Pfeiffer, H. Kuzmany, T. Gemming and B. Büchner, High quality double wall carbon nanotubes with a defined diameter distribution by chemical vapor deposition from alcohol, Carbon 44 (2006), 3177-3182.

[8] Shuhei Inoue, Takeshi Nakajima and Yoshihiro Kikuchi, Synthesis of single-wall carbon nanotubes from alcohol using Fe/Co, Mo/Co, Rh/Pd catalysts, Chemical Physics Letters 406 (2005), 184-187.

[9] Shuhei Inoue and Yoshihiro Kikuchi, Diameter control and growth mechanism of single-walled carbon nanotubes, Chemical Physics Letters 410 (2005), 209-212.

10] Lianxi Zheng, Xiaozhou Liao and Yuntian T. Zhu, Parametric study of carbon nanotube growth via cobalt-catalyzed ethanol decomposition, Materials Letters 60 (2006), 1968-1972.

[11] D. Nishide, H. Kataura, S. Suzuki, S. Okubo and Y. Achiba, Growth of singlewall carbon nanotubes from ethanol vapour on cobalt particles produced by pulsed laser vaporization, Chemical Physics Letters 392 (2004), 309-313.

[12] G. Ortega-Cervantez, G. Rueda-Morales and J. Ortiz-López, Catalytic CVD production of carbon nanotubes using ethanol, Microelectronics Journal 36 (2005), 495-498.

[13] Luciano Andrey Montoro, Paola Corio and José Maurício Rosolen, A comparative study of alcohols and ketones as carbon precursor for multiwalled carbon nanotube growth, Carbon 45 (2007), 1234-1241.

[14] Yoon Huh, Malcolm L. H. Green, Young Heon Kim, Jeong Yong Lee and Cheol Jin Lee, Control of carbon nanotube growth using cobalt nanoparticles as catalyst, Applied Surface Science 249 (2005), 145-150.

[15] Young Min Shin, Seung Yol Jeong, Hee Jin Jeong, Sung Jin Eum, Cheol Woong Yang, Chong Yun Park and Young Hee Lee, Influence of morphology of catalyst thin film on vertically aligned carbon nanotube growth, Journal of Crystal Growth 271 (2004), 81-89.

[16] Hanming Liu, Xiao Wang, Pengfei Fang, Shaojie Wang, Xiang Qi, Chunx Pan and Guangyoung Xie, Functionalization of multiwalled carbon nanotubes grafted with self-generated functional groups and their polyamide composites, Carbon 48 (2010), 721-729.

[17] S. Porro, S. Musso, M. Vinante, L. Vanzetti, M. Anderle, F. Trotta and A. Tagliaferro, Purification of carbon nanotubes grown by termal CVD, Physica E 37 (2007), 58-61.

https://cimav.repositorioinstitucional.mx/jspui/

[18] HSC 5.1. Chemistry. http://www.esm-software.com/hsc/

[19] Albert Nashibulin, David P. Brown, Paula Queipo, David Gonzalez, Hua Jiang and Esko I. Kauppinen, An essencial role of CO2 and H2O during single-walled CNT synthesis from carbon monoxide.

[20] Wu Zhang, Dekun Ma, Jianwei Liu, Lingfen Kong, Weichao Yu and Yitai Qian, Solvothermal synthesis of carbon nanotubes by metal oxide and ethanol at mild temperature, Letters to the Editor/Carbon 42 (2004), 2329-2366.

[21] M. Pérez Cabrero, E. Romeo, A. Monzón, A. Guerrero-Ruíz and I. Rodríguez Ramos, Growing mechanism of CNTs: a kinetics approach, Journal of Catalysis 224 (2004), 197-205.